Applied Thermal Engineering 87 (2015) 539–546

Contents lists available at ScienceDirect

Applied Thermal Engineering

journal homepage: www.elsevier.com/locate/apthermeng

Research paper

Some aspects of stabilization and structure of laminar premixed hydrogen-air flames in a microchannel

Swarup Y. Jejurkar*, D.P. Mishra

Combustion Laboratory, Department of Aerospace Engineering, Indian Institute of Technology Kanpur 208 016 India

HIGHLIGHTS

- homogeneous ignition of flame by continuous ignition mechanism.
- thermal diffusion of H_2 at the leading edge affects flame structure.
- twin-peaked heat release profile for rich flame.
- unravels role of OH in reaction kinetics of rich flame.

GRAPHICAL ABSTRACT

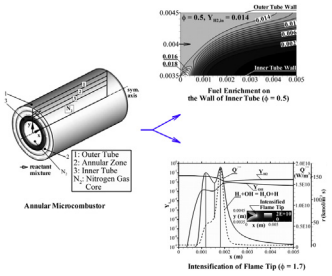

ARTICLE INFO

Article history:
Received 24 February 2015
Accepted 20 May 2015
Available online 30 May 2015

Keywords:
Hydrogen
Flame structure
Microcombustion
Thermal diffusion

ABSTRACT

In the present paper, flame stabilization and structure are investigated numerically for non-adiabatic hydrogen-air flames at different equivalence ratios and inlet velocities. A cylindrical microcombustor in which combustion occurs in the annular region between two concentric tubes is investigated. The inner hollow tube contains static nitrogen gas and this combination acts as a thermal reservoir that stores and recirculates heat to the incoming mixture. Investigations are carried out using detailed numerical model incorporating two-dimensional transport, thermal radiation, multi-step kinetics, and conjugate heat transfer. Flame is sustained by the continuous ignition mechanism activated by an uninterrupted temperature field between gas mixture and wall developing at steady state. Heat losses from flame resulted in a crossover temperature higher than that of the lean-limit and stoichiometric free flames due to slow radical build-up. Thermal diffusion of hydrogen is shown to be responsible for enhancing the burning intensity of leading edge. Diffusion and reaction kinetics at the flame tip result in twin-peaked heat release rate distribution, most prominently for fuel rich flame ($\phi = 1.7$).

1. Introduction

Microcombustion is a potential power source for miniature devices. However, issues such as flame stabilization [1–3], flame-wall interaction [4], and reaction kinetics [5] in these devices need to be handled for successful operation. Increased flame-wall thermal coupling in a narrow passage affects reaction kinetics [5]. Branching by $H_2 + O = H + OH$ and $H + O_2 = O + OH$ dominates propagation by $HO_2 + H = 2OH$ in lean ($\phi = 0.5$) hydrogen flame at microscale [5]. Kagan and Sivashinsky [6] used reaction-diffusion model of two-dimensional (2D) flame stabilized at the junction of hot and cold sides to study the effects of radiation losses on tip opening for Lewis number ($Le = \alpha/D$) equal to 0.5. More fuel leaked from tip and burnt as diffusion flame near the ruptured tip as heat losses and inlet velocity increased. Conduction losses played no role

* Corresponding author. Tel.: +91 512 259 7125.
E-mail addresses: flowdyna@gmail.com (S.Y. Jejurkar), mishra@iitk.ac.in (D.P. Mishra).

http://dx.doi.org/10.1016/j.applthermaleng.2015.05.053
1359-4311/

in tip opening but caused global quenching for small gaps [6]. Internal radiation could also inhibit quenching in the absence of axial conduction [7]. Slow displacement of flame stabilized on hot wall of refractory tube in response to perturbations in the wall boundary conditions has been demonstrated [8]. Fu et al. [9] numerically showed that balance between heat release and heat transfer influenced the location of flame stabilization in adiabatic narrow tube.

In microcombustion, 2D flame could stabilize in shear flow with "stagnation streamline" [3] for given velocity gradient in radial direction due to increased flame thickness in the presence of heat losses. Flame can also thicken by improved preheating [9] in microcombustor. According to Kessler and Short [4], thermal feedback would not affect upstream movement of flame in the high velocity regime (flame propagation velocity ~ incoming mixture velocity) as heat transfer rate would lag behind the flame displacement rate when starting from cold conditions. However, flame displacement after attachment to wall depends upon wall heat conduction and wall thermal conductivity (k_{wall}) determines extent of upstream displacement prior to stabilization near inlet [10,11].

Much on the mechanism of flame stabilization and flame structure near the hot walls of microcombustors remains unknown. The principle aim of this study is to address structural aspects of hydrogen-air laminar premixed flames with the help of numerical simulations and address these unknown issues. Flame stabilization mechanism is discussed in the beginning, followed by flame structure near walls and tip. Flame-wall interactions are explored with the help of dominant reactions. Differences in the structure of flames stabilized in microcombustor and the canonical flat flames are explored, with reference to conditions of heat losses.

2. Annular microcombustor

Results are obtained on annular microcombustor (Fig. 1) consisting of static nitrogen (N_2) gas stored in a sealed hollow inner tube (1 mm thick, inner diameter 5 mm, length 20 mm). The intention is to store the gas and not recycle it. Part of the exhaust gas mixture could also be used instead of N_2. However, this variation is not considered in the present study. Consequently, nitrogen is stored under static conditions in the hollow inner tube. Concentric outer shell has 1 mm thickness, inner diameter 9 mm, and length 20 mm. Annular reaction zone (ARZ) thus formed is 1 mm wide. It should be noted that flame is free to stabilize anywhere in the ARZ, depending upon the inlet conditions and prevalent thermal state. Overall volume and surface area/volume based on the external wall of outer shell are 1.9×10^{-6} m^3 and 364 m^{-1}, respectively.

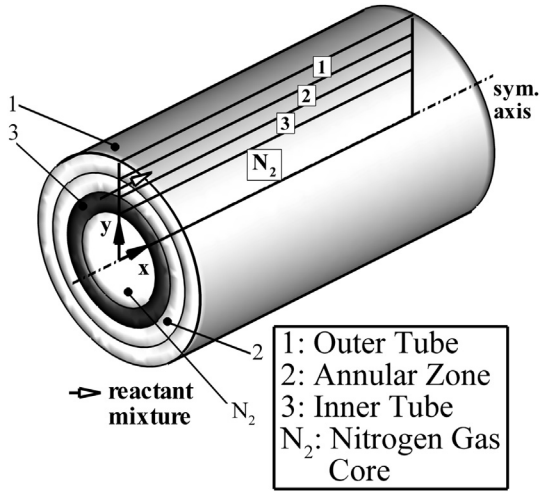

Fig. 1. Schematic of annular microcombustor and axisymmetric computational domain.

3. Numerical procedure and error analysis

3.1. Numerical model and boundary conditions

Eqs. (1)–(6) constitute general mathematical formulation that is transformed appropriately for the axisymmetric computational domain shown in Fig. 1 in the $+x+y$ plane of Cartesian coordinate space. Transport of isotropically scattered radiation intensity (I) in gray media (walls and gas) is modeled by discrete ordinates method (DOM).

$$\frac{\partial \rho}{\partial t} + \nabla \cdot (\rho V) = 0 \tag{1}$$

$$\frac{\partial (\rho V)}{\partial t} + \nabla \cdot (\rho V V) = -\nabla P + \nabla \cdot \bar{\bar{\tau}} \tag{2}$$

$$\frac{\partial (\rho E)}{\partial t} + \nabla \cdot [V(\rho E + P)] = \nabla \cdot \left[k \nabla T - \sum_{i=1}^{n} h_i J_i + (\bar{\bar{\tau}} \cdot V) \right] + S_r + S_{rad} \tag{3}$$

$$\frac{\partial (\rho h)}{\partial t} = \nabla \cdot (k \nabla T) + S_{rad} \tag{4}$$

$$\frac{\partial (\rho Y_i)}{\partial t} + \nabla \cdot (\rho V Y_i) = -\nabla \cdot J_i + r_i \tag{5}$$

$$\nabla \cdot (I(r,s)s) = -(\alpha + \sigma_s) I(r,s) + \alpha n_r^2 \frac{\sigma T^4}{\pi} + \frac{\sigma_s}{4\pi} \int_0^{4\pi} I(r,s) d\Omega' \tag{6}$$

Eqs. (1) and (2) are the continuity and momentum transport equations. Two energy equations, Eqs. (3) and (4) are written, one each for gas and solid phases, respectively. Energy equation for gas phase is written for energy, E that accounts for sensible enthalpy of mixture and kinetic energy ($E = h - (P/\rho) + (V^2/2)$. Sensible enthalpy of mixture is written as a mass fraction weighted sum of species enthalpies ($h = \sum_j Y_j h_j + P/\rho$ and $h_j = \int_{T_{ref}}^{T} C_{P,j} dT$) referenced to $T_{ref} = 298.15$ K. Note that this equation accounts for sources of energy due to chemical reaction (S_r) and radiation (S_{rad}). These volumetric sources are estimated from separate sub-models in terms of multi-step kinetics and DOM. Heat conduction, species diffusion, and viscous dissipation terms are accounted in Eq. (3). Energy equation for solid phase includes heat conduction and thermal radiation within the walls of microcombustor. Species transport equation written in Eq. (5) includes species transport by diffusion flux and formation/destruction by multiple reactions. Species transport equations are solved for 8 species (H, H_2, O, O_2, OH, HO_2, H_2O_2, and H_2O). Nitrogen, the most abundant species in the mixture, is taken as the ninth species and the mass fraction of nitrogen is obtained from the consistency condition, $Y_{N_2} = 1 - \sum_{i=1}^{n-1} Y_i$. Reaction rate ($r_i$) is $r_i = MW_i \sum_{r=1}^{n_R} R_{i,r}$. $R_{i,r}$ is the molar rate of rth reaction of ith species computed using Konnov's multistep mechanism [12]. Surface kinetics, viz. wall activity and radical quenching on the wall, are not considered here and only homogeneous reactions are included.